Physics of noise in quantum-confined field-effect transistors

F. Green
GaAs IC Prototyping Facility, CSIRO Division of Radiophysics, P.O. Box 76, Epping New South Wales 2121, Australia

M. J. Chivers
Department of Electrical and Electronic Engineering, University of Western Australia, Nedlands Western Australia 6009, Australia

(Received 16 October 1995; revised manuscript received 7 March 1996)

We present a microscopic theory of nonequilibrium current noise in quantum-well-confined, two-dimensional, metallic conduction bands, systems that are central to the operation of high-performance III-V heterojunction transistors. Using a Boltzmann-Green-function approach, we give a unified description of both transport and dynamic fluctuations for these structures and provide a fully microscopic analysis of Fukui's noise constant for heterojunction devices. [S0163-1829(96)00732-1]

I. INTRODUCTION

High-electron-mobility transistors (HEMTs), built on III-V heterostructures, are crucial to millimeter-wave technology. In their low noise, as well as in their gain and power handling, HEMTs significantly outperform earlier field-effect designs.[1]

The influence of microscopic structure on gain is well understood in HEMTs,[2] but its effect on noise properties is not. Much of the noise-modeling literature is based on adaptations of classical circuit theory or its hydrodynamic extensions[3,4] and cannot address current fluctuations in quantum wells. For example, quantum-well confinement must affect the *scale* of intrinsic carrier noise just as it affects intrinsic gain,[5] but this has not been analyzed before now. Furthermore, most device models fail to treat transport and noise in a mutually consistent way.

Here we propose a fully consistent, microscopic model of noise in heterojunction devices. Carrier fluctuations are described by Green-function solutions to the Boltzmann equation, an approach developed for classical electrons in GaAs by Stanton and Wilkins[6–8] (SW). In bulk, lightly doped III-V materials, the SW model successfully captures the character of high-field transport and noise.[7]

Our contribution is twofold. First, we reformulate the Boltzmann-Green-function approach to describe nonequilibrium fluctuations in degenerate HEMT channels. Second, we use this method to give an alternative explanation of noise suppression in the source and drain access regions of the HEMT channel, with direct implications for the practical design of low-noise heterostructures.

For noise in the high-field gate region, we offer a simpler alternative to the more formal quantum-kinetic treatments[9–11] and to stochastic simulations.[12–15] At the same time, we use microscopic arguments beyond the scope of semiempirical models.[4,16,17]

Commonly, the HEMT access regions are believed to suppress overall noise through high mobility, reducing the scale of the thermal fluctuations. By contrast, we demonstrate that high mobility cannot account for noise reduction in these low-field regions. Rather, the noise physics there is dominated by two quantum effects: screening and degeneracy.

In Sec. II we describe our theory of fluctuations in degenerate, two-dimensional electron gases (2DEGs) and discuss the role of quantum-confined screening, which distinguishes HEMTs from bulk devices. In Sec. III we apply the theory to a simple model 2DEG, illustrating core concepts. We then give a microscopic interpretation of the device noise figure and the empirical Fukui noise coefficient.[17] In Sec. IV we present numerical calculations of the noise figure, with the focus on quantum-confinement physics. Finally, in Sec. V we preview the extension of our method to multiband scattering for more realistic device-noise modeling. We also briefly survey our semiclassical approach in the context of quantum-kinetic theory.

II. THEORY

In the theory of classical Boltzmann propagators,[6] one cannot distinguish between Maxwellian distribution functions and their fluctuations; in Fermi systems, however, the distinction is crucial. In this section we give a prescription for evolving the nonequilibrium fluctuation structure in terms of Boltzmann-Green functions.

A. Transport equation

We need the distribution function $f_\sigma(\mathbf{r},\mathbf{k},t)$ over electron spin σ, position $\mathbf{r}$, and wave vector $\mathbf{k}$ for time t. All the local one-body properties are traces over spin and wave vector, for example, the 2DEG density $n_s(\mathbf{r},t)$ and the drift velocity $\overline{\mathbf{v}(\mathbf{r},t)}$. Following SW,[6] we make a simple relaxation-time ansatz for the collision term of the Boltzmann equation

$$\left[\frac{\partial}{\partial t}+\mathbf{v}_\mathbf{k}\cdot\frac{\partial}{\partial \mathbf{r}}-\frac{q\mathbf{E}}{\hbar}\cdot\frac{\partial}{\partial \mathbf{k}}\right]f(\mathbf{r},\mathbf{k},t)$$
$$=-\frac{f(\mathbf{r},\mathbf{k},t)-A[f(t)]f^{\mathrm{eq}}(\mathbf{r},k)}{\tau_{\mathrm{in}}(k)}$$
$$-\frac{f(\mathbf{r},\mathbf{k},t)-\overline{f(\mathbf{r},\mathbf{k},t)}^{\phi}}{\tau_{\mathrm{el}}(k)}. \tag{1}$$

The first part of the collision term models inelastic processes, which will also dominate the noise spectrum. This inelastic term is not manifestly particle conserving because

the collision time $\tau_{\rm in}(k)$ is momentum dependent. Conservation is restored via the scale factor $A[f(t)]$ multiplying the equilibrium function $f^{\rm eq}$ and chosen to keep n_s invariant. The second collision term represents elastic scattering, which tends to restore angular isotropy; the distortion is measured against the angle average $\overline{f(\mathbf{r},\mathbf{k},t)}^{\phi}$ in $\mathbf{k}$ space. Elastic collisions set up cross correlations between x- and y-directed motions.

Here we specialize to intraband transport in the ground state of a uniform 2DEG. The space-gradient term is absent from Eq. (1), and we define the constant field as $\mathbf{E}=-\mathcal{E}\hat{\mathbf{x}}$. The distribution $f(\mathbf{k},t)$ then simulates a HEMT channel in the long-gate limit.

Note that our methodology is not inherently restricted to this special case. In complete form it admits the same detailed effects of intervalley scattering[7] and inhomogeneity[18] as the classical description, but now making these effects applicable to metallic electrons.

Apart from Coulomb screening, included in $\mathcal{E}$ through the random-phase approximation,[19] the other major effect for inclusion is degeneracy. This dominates the equilibrium free energy in the density range of device physics ($\sim 10^{12}$ cm^{-2}) and will also govern the nonequilibrium 2DEG.

B. Steady-state fluctuations

Calculation of noise requires knowledge of steady-state 2DEG behavior. The steady-state solution $f(\mathbf{k})\equiv f(\mathbf{k},t\rightarrow\infty)$ is proportional to a particular solution of Eq. (1) with $A[f]=1$; let this be $f_1(\mathbf{k})$. Though not particle conserving in general, f_1 determines the physical solution

$$f(\mathbf{k})=A[f]f_1(\mathbf{k})=\frac{\langle f^{\rm eq}\rangle}{\langle f_1\rangle}f_1(\mathbf{k}), \tag{2}$$

where $\langle f\rangle$ is the sum over the wave vector and spin state space; $\langle f\rangle=\Omega^{-1}\Sigma_{\mathbf{k},\sigma}f_\sigma(\mathbf{k})$, where Ω is the area of the active 2DEG. The conservation constraint $\langle f\rangle=\langle f^{\rm eq}\rangle=n_s$ implies the more general relation $A[f]=\langle f/\tau_{\rm in}\rangle/\langle f^{\rm eq}/\tau_{\rm in}\rangle$. This shows the direct link between the choice of inelastic collision time and conservation.

A density change in the underlying equilibrium state perturbs the Fermi-Dirac distribution. In turn, this will propagate adiabatically to the nonequilibrium steady state. The nonequilibrium perturbation obeys an equation of motion derivable from the structure of Eq. (1), which describes the steady-state Boltzmann-Green function

$$R_{\sigma\sigma'}(\mathbf{k},\mathbf{k}')\equiv\frac{\delta f_\sigma(\mathbf{k})}{\delta f^{\rm eq}_{\sigma'}(\mathbf{k}')}. \tag{3}$$

It is convenient to get the variation of f with respect to an arbitrary change in $f^{\rm eq}$, from Eq. (2):

$$R_{\sigma\sigma'}(\mathbf{k},\mathbf{k}')=\frac{f_{1\sigma}(\mathbf{k})}{\langle f_1\rangle}+\frac{\langle f^{\rm eq}\rangle}{\langle f_1\rangle}\left(\frac{\delta f_{1\sigma}(\mathbf{k})}{\delta f^{\rm eq}_{\sigma'}(\mathbf{k}')}-\frac{f_{1\sigma}(\mathbf{k})}{\langle f_1\rangle}\left\langle\frac{\delta f_1}{\delta f^{\rm eq}_{\sigma'}(\mathbf{k}')}\right\rangle\right). \tag{4}$$

The fluctuation of the equilibrium state is determined by the change in $f^{\rm eq}(k')$ in response to a change in the Fermi level:[20]

$$\Delta f^{\rm eq}_\sigma(k)\equiv k_BT\frac{\partial f^{\rm eq}_\sigma(k)}{\partial E_F}. \tag{5}$$

Hence the contribution to the nonequilibrium fluctuation in state $\mathbf{k}\sigma$, from the fluctuation in the underlying equilibrium state $\mathbf{k}'\sigma'$, is

$$\Delta f^{(2)}_{\sigma\sigma'}(\mathbf{k},\mathbf{k}')\equiv R_{\sigma\sigma'}(\mathbf{k},\mathbf{k}')\Delta f^{\rm eq}_{\sigma'}(k'). \tag{6}$$

The Boltzmann-Green function builds up the steady-state fluctuations in much the same way that, in many-body perturbation theory, the ground-state fluctuations are generated by the particle-hole vertex.[21]

The fluctuation in $f_\sigma(\mathbf{k})$ is the trace of $\Delta f^{(2)}_{\sigma\sigma'}(\mathbf{k},\mathbf{k}')$:

$$\Delta f_\sigma(\mathbf{k})\equiv\langle\Delta f^{(2)}(\mathbf{k},\mathbf{k}')\rangle'=\frac{1}{\Omega}\sum_{\mathbf{k}',\sigma'}\Delta f^{(2)}_{\sigma\sigma'}(\mathbf{k},\mathbf{k}'). \tag{7}$$

Just as $\partial f^{\rm eq}(k)/\partial E_F=\Delta f^{\rm eq}(k)/k_BT$ is the density-density correlation function for a free-electron liquid in the static long-wavelength limit,[21] so $\Delta f(\mathbf{k})/k_BT$ is its nonequilibrium counterpart, calculated in our semiclassical approximation. For a degenerate system with a constant relaxation time, the structure associated with Eq. (6) recovers the Johnson-Nyquist noise temperature formula in the low-field limit [see Sec. III, Eqs. (32) and (37)]. As expected, the anticorrelation generated by Pauli exclusion is manifested in the fluctuations since $\Delta f^{\rm eq}=f^{\rm eq}(1-f^{\rm eq})$.

The steady-state description is completed by specifying the equation for the auxiliary propagator $\delta f_1(\mathbf{k})/\delta f^{\rm eq}(\mathbf{k}')$. This is generated by varying both sides of Eq. (1) while $A[f_1]$ is forced to unity:

$$\frac{q\mathcal{E}}{\hbar}\frac{\partial}{\partial k_x}\frac{\delta f_{1\sigma}(\mathbf{k})}{\delta f^{\rm eq}_{\sigma'}(\mathbf{k}')}=-\frac{1}{\tau_{\rm in}(k)}\left(\frac{\delta f_{1\sigma}(\mathbf{k})}{\delta f^{\rm eq}_{\sigma'}(\mathbf{k}')}-\Omega\,\delta_{\mathbf{k}\mathbf{k}'}\delta_{\sigma\sigma'}\right)-\frac{1}{\tau_{\rm el}(k)}\left(\frac{\delta f_{1\sigma}(\mathbf{k})}{\delta f^{\rm eq}_{\sigma'}(\mathbf{k}')}-\frac{\overline{\delta f_{1\sigma}(\mathbf{k})}^{\phi}}{\delta f^{\rm eq}_{\sigma'}(\mathbf{k}')}\right). \tag{8}$$

C. Dynamical fluctuations

We have characterized the steady-state fluctuations as the adiabatic mapping of the spontaneous thermal fluctuations of the equilibrium system. These excursions of $f(\mathbf{k})$ out of the background steady state will propagate in momentum space according to the time-dependent Eq. (1). Equivalently, a dynamic fluctuation $\Delta f(\mathbf{k},t)$ referred to an arbitrary starting time t_0 will be seen as having developed from the distribution of spontaneous nonequilibrium fluctuations at $t=t_0$ so that initially $\Delta f(\mathbf{k}',t_0)=\Delta f(\mathbf{k}')$. This leads to the retarded Boltzmann-Green function [where $\theta(t)$ is the unit step]

$$\mathcal{R}_{\sigma\sigma'}(\mathbf{k},\mathbf{k}';t-t_0)\equiv\theta(t-t_0^+)\frac{\delta f_\sigma(\mathbf{k},t)}{\delta f_{\sigma'}(\mathbf{k}',t_0)}. \tag{9}$$

Its equation of motion is obtained by taking variations on both sides of Eq. (1):

$$\frac{\partial \mathcal{R}}{\partial t}+\frac{q\mathcal{E}}{\hbar}\frac{\partial \mathcal{R}}{\partial k_x}=\delta(t-t_0^+)\mathcal{R}_{\sigma\sigma'}(\mathbf{k},\mathbf{k}';0^+)-\frac{1}{\tau_{\rm in}(k)}\left(\mathcal{R}-\frac{\langle \mathcal{R}/\tau_{\rm in}\rangle}{\langle f^{\rm eq}/\tau_{\rm in}\rangle}f^{\rm eq}(k)\right)-\frac{1}{\tau_{\rm el}(k)}(\mathcal{R}-\overline{\mathcal{R}^{\phi}}), \tag{10}$$

with initial value $\mathcal{R}_{\sigma\sigma'}(\mathbf{k},\mathbf{k}';0^+)=\Omega\,\delta_{\mathbf{k}\mathbf{k}'}\delta_{\sigma\sigma'}$.

To determine the natural time evolution of Δf, define the time-dependent density-density fluctuation

$$\Delta f^{(2)}_{\sigma\sigma'}(\mathbf{k},\mathbf{k}';t)\equiv\mathcal{R}_{\sigma\sigma'}(\mathbf{k},\mathbf{k}';t)\Delta f_{\sigma'}(\mathbf{k}'). \tag{11}$$

Knowledge of $\Delta f^{(2)}(\mathbf{k},\mathbf{k}';t)$ now provides every time-dependent correlation of physical interest. In particular, the mean-square velocity fluctuation per electron is defined by

$$\begin{aligned}D_{ij}(t,\mathcal{E})&=\frac{1}{n_s}\langle\langle(v_i-\overline{v_i})(v_j'-\overline{v_j})\Delta f^{(2)}(t)\rangle\rangle'\\&=\frac{1}{n_s\Omega^2}\frac{1}{\Omega^2}\sum_{\mathbf{k},\sigma}\sum_{\mathbf{k}',\sigma'}[(v_i)_{\mathbf{k}}-\overline{v_i}][(v_j)_{\mathbf{k}'}-\overline{v_j}]\\&\quad\times\Delta f^{(2)}_{\sigma\sigma'}(\mathbf{k},\mathbf{k}';t),\end{aligned} \tag{12}$$

where labels i,j can be in either the x or the y direction with respect to the driving field and the drift velocity is

$$\overline{v_i}(\mathcal{E})\equiv\frac{1}{n_s}\langle v_i f\rangle=\frac{1}{n_s}\left\langle\frac{1}{\hbar}\frac{\partial E(k)}{\partial k_i}f\right\rangle. \tag{13}$$

The dynamical noise temperature is obtained from Eq. (12) by standard manipulations. In the frequency domain, the velocity fluctuation is[22]

$$\hat{D}_{ij}(\omega,\mathcal{E})=\int_0^\infty dt\cos(\omega t)D_{ij}(t,\mathcal{E}). \tag{14}$$

Using parallel expressions of the current-current spectral density[22] — one microscopic, the other macroscopic — the measurable noise temperature T_n is obtained in terms of $\hat{D}_{xx}$ and the differential mobility $\mu=\partial\overline{v_x}/\partial\mathcal{E}$, both calculable within the formalism:

$$T_{n[xx]}(\omega,\mathcal{E})=\frac{q\hat{D}_{xx}(\omega,\mathcal{E})}{k_B\mu(\omega,\mathcal{E})}. \tag{15}$$

Since typical collision rates in the 2DEG channel will be of the order of 10^{-13} s, much shorter than millimeter-wave time scales ($\sim10^{-11}$ s), we will take the static limit of all dynamical expressions.

D. Quantum confinement and screening

In addition to depending on the Fermi level, the 2DEG equilibrium distribution $f^{\rm eq}(k)$ also depends on the quantization energy of its quantum-well subband. The specific functional form of the subband energies varies with the nature of the heterostructure and its quantum well. For our ground-state-only model, let the energy be $E_0(n_s)$. The equilibrium distribution is

$$f^{\rm eq}(k)=\frac{1}{1+\exp\{[E(k)+E_0(n_s)-E_F]/k_BT\}}. \tag{16}$$

Assuming for simplicity that $E(k)$ is parabolic, the integrated 2DEG density is

$$n_s=n_s^*\ln(1+\exp\{[E_F-E_0(n_s)]/k_BT\}), \tag{17}$$

where $n_s^*=m^*k_BT/\pi\hbar^2$ and m^* is the effective electron mass. We now obtain the total response of $f^{\rm eq}$ and n_s to a change in the Fermi level. The change in n_s with respect to E_F alone, keeping E_0 fixed, determines the free-electron density fluctuation

$$\Delta n_s=k_BT\frac{\partial n_s}{\partial E_F}=n_s^*(1-e^{-n_s/n_s^*}). \tag{18}$$

The complete derivative of n_s with respect to E_F is then

$$\frac{\delta n_s}{\delta E_F}=\left(1-\frac{dE_0}{dn_s}\frac{\delta n_s}{\delta E_F}\right)\frac{\partial n_s}{\partial E_F}=\left(1+\frac{\Delta n_s}{k_BT}\frac{dE_0}{dn_s}\right)^{-1}\frac{\Delta n_s}{k_BT}. \tag{19}$$

Similarly, for $f^{\rm eq}(k)$,

$$\frac{\delta f^{\rm eq}(k)}{\delta E_F}=\left(1+\frac{\Delta n_s}{k_BT}\frac{dE_0}{dn_s}\right)^{-1}\frac{\partial f^{\rm eq}(k)}{\partial E_F}. \tag{20}$$

This is the density-density correlation in the ground-state subband at equilibrium.[23]

Let γ_s denote the first factor on the right-hand side of Eq. (20) and define the total density-density fluctuation

$$\tilde{\Delta}f^{\rm eq}(k)\equiv k_BT\frac{\delta f^{\rm eq}(k)}{\delta E_F}=\gamma_s\Delta f^{\rm eq}(k). \tag{21}$$

Figure 1 plots the density and fluctuation profiles for a typical $In_xGa_{1-x}As$ HEMT as a function of gate-bias voltage and shows that the renormalization of the density-density correlation can be large, up to a factor of 3 down on the unscreened quantity. This comes from self-consistent screening of the potential confining the 2DEG and is the Thomas-Fermi response of the strongly quantized electrons, along the axis of confinement. A perturbation (systematic or random) changes the value of the local density, displacing the local Fermi level; self-screening provides negative feedback, which reduces the observable fluctuations. This is analogous to space-charge-induced suppression of shot noise, familiar from the physics of vacuum tubes.[8,24]

For noise behavior in heterostructures, the most important implication of Eq. (21) is a rescaling of all expressions linear in the unscreened fluctuation $\Delta f^{\rm eq}$. In particular, this alters the quantitative content of Eqs. (6), (7), (11), and (12) for the nonequilibrium fluctuations.

The noise temperature is therefore suppressed below its bare counterpart, by the factor γ_s [see Eq. (15)]:

$$\tilde{T}_n(\omega,\mathcal{E})=\gamma_sT_n(\omega,\mathcal{E}). \tag{22}$$

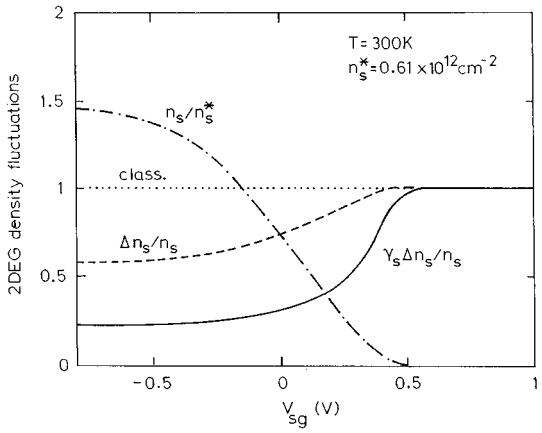

FIG. 1. Density fluctuations of a 2DEG in a pseudomorphic quantum well, 15 nm wide, at $T=300$ K (alloy composition $Al_{0.23}Ga_{0.77}As/In_{0.15}Ga_{0.85}As/GaAs$). Dot-dashed line, density in dimensionless units as a function of gate-bias potential; dashed line, fractional density fluctuation without screening suppression, equivalent to the degeneracy factor $\Delta n_s/n_s$ [carriers, strongly degenerate for $V_{sg}<0$, behave classically in the low-density limit (large positive V_{sg})]; full line, fractional fluctuation including screening suppression, equivalent to static electron susceptibility times k_BT; dots, classical fluctuations, with no degeneracy or screening. Screening suppression acts *only* in the presence of self-consistent bound states.

Screening suppression is also reminiscent of the noise coefficient of metal-oxide-semiconductor transistors, which alters the usual Nyquist expression for drift-diffusion noise in the inversion layer.[25]

In addition to confinement-induced screening, a different kind of screening arises from short-range interactions within the 2DEG, namely, exchange corrections to the random-phase approximation and multiparticle scattering. These set up the exchange-correlation hole,[26] a zone of electron depletion around any given electron reducing the magnitude of the free-electron fluctuations. This screening mechanism is dominant in the zero-temperature limit, but for the finite-temperature 2DEG its effect is minor (at most 5%) according to estimates based on the static-local-field correction.[26]

The considerations we have set out here fit the physical structure of a HEMT; the gate-control voltage V_{sg}, coupling to $\tilde{\Delta} f(\mathbf{k})$ by modulating the Fermi level, is equally effective in the differential channel-to-gate capacitance C_{sg} and the transconductance g_m. This is seen from the unscreened expressions[27]

$$C_{sg}=-\Omega q\left\langle \frac{\delta f}{\delta V_{sg}}(\omega)\right\rangle =-\frac{\Omega q}{k_BT}\langle \Delta f(\omega)\rangle \frac{\delta E_F}{\delta V_{sg}}(\omega), \tag{23}$$

$$g_m=-\frac{\Omega q}{L_g k_B T}\langle v_x \Delta f(\omega)\rangle \frac{\delta E_F}{\delta V_{sg}}(\omega) \tag{24}$$

over length L_g for the active gate region. The derivative $\delta E_F/\delta V_{sg}$ comes from solving the standard Poisson problem in the $Al_xGa_{1-x}As$ donor layer above the quantum well.[5]

The 2DEG fluctuations provide the fundamental basis for g_m, C_{sg}, and T_n. Together with the action of screening-induced suppression on all of these parameters, this underlines the importance of developing a seamless approach to modeling the HEMT response. Both the stationary and transient aspects of device performance should be treated on an equal footing rather than be modeled separately and reconciled only after the fact.

III. APPLICATIONS

A. Constant mobility model

We now examine the simplest example of our relaxation-time formalism. We assume parabolic dispersion and a constant inelastic collision time, with no elastic scattering: let $\tau_{in}=\tau$ and $\tau_{el}=\infty$. The steady-state solution to Eq. (1) is[8]

$$f(\mathbf{k})=\lambda\int_{-\infty}^{k_x} dk_x' e^{-\lambda(k_x-k_x')} f^{eq}(k'), \tag{25}$$

where $\lambda=\hbar/(q\mathcal{E}\tau)$ and $k_y'=k_y$. The drift velocity is calculated by integrating f over $\mathbf{k}$:

$$\overline{v_x}=\frac{\hbar}{m^*}\frac{\langle k_x f\rangle}{n_s}=\mu\mathcal{E}. \tag{26}$$

Here $\mu=\hbar/(m^*\lambda\mathcal{E})=q\tau/m^*$.

The fluctuation $\Delta f(\mathbf{k})$ follows directly:

$$\Delta f(\mathbf{k})=\lambda\int_{-\infty}^{k_x} dk_x' e^{-\lambda(k_x-k_x')}\Delta f^{eq}(k'). \tag{27}$$

Figures 2 – 4 show $f(\mathbf{k})$ and $\Delta f(\mathbf{k})$ for a range of situations. In Fig. 2 the equilibrium and steady-state distributions are plotted at density $n_s=10^{10}$ cm^{-2} and temperature $T=300$ K, in the classical limit. Since $f^{eq}(k)$ is Maxwellian, we have $\Delta f^{eq}(k)=f^{eq}(k)$. Therefore Eqs. (25) and (27) give identical results, shown in Fig. 2(b) for a driving field $\mathcal{E}=5$ kV cm^{-1}. A high-momentum exponential (not Gaussian) tail develops in $f(\mathbf{k})$ along the field direction.

Figures 3 and 4, for $n_s=10^{12}$ cm^{-2}, show strong degeneracy effects. There is a rich structure in Δf^{eq} around the 2D Fermi ''surface'' [Fig. 3(b)]. Figure 4 displays the distortion of the distributions subject to the same field as Fig. 2(b). Because the volumes n_s and Δn_s under each plot are conserved and much more weight goes into the high-momentum tails, the peaks fall below their equilibrium values. For $\Delta f(\mathbf{k})$ [Fig. 4(b)], the highly distorted, remnant Fermi surface is visible.

The dynamical expectation values needed for the noise depend on a set of steady-state integrals, which give

$$\langle \Delta f\rangle=\Delta n_s, \tag{28}$$

$$\langle v_x \Delta f\rangle=\overline{v_x}\Delta n_s, \tag{29}$$

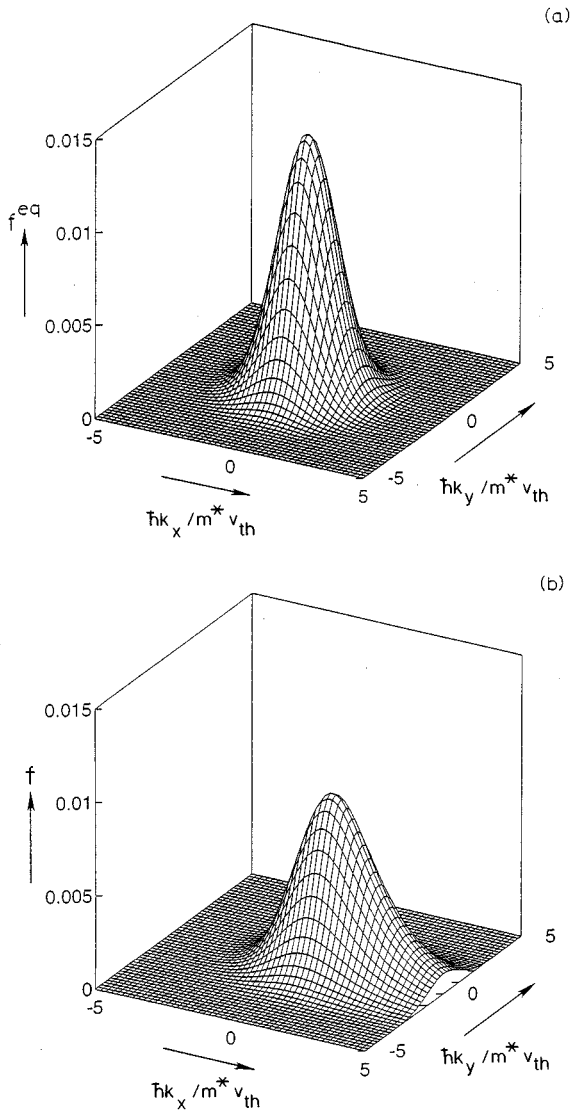

FIG. 2. Classical 2DEG distributions. (a) Equilibrium distribution in momentum space, at a density 10^{10} cm^{-2}, is its own fluctuation. The ambient temperature is 300 K, and mobility is 8000 cm^2 V^{-1}s^{-1}. (Momenta are in thermal units.) (b) Classical nonequilibrium distribution in a driving field of 5 kV cm^{-1} along the x direction.

$$\langle v_x^2 \Delta f\rangle = 2\left(\frac{\hbar}{m^*}\right)^2 \int_{-\infty}^{\infty}\frac{dk_y'}{2\pi}\int_{-\infty}^{\infty}\frac{dk_x'}{2\pi}\Delta f^{\mathrm{eq}}(k') \times \int_{k_x'}^{\infty} dk_x k_x^2 \lambda e^{-\lambda(k_x-k_x')} = v_{\mathrm{th}}^2 n_s + 2\overline{v_x}^2 \Delta n_s, \tag{30}$$

with $v_{\mathrm{th}}^2 \equiv k_B T/m^*$. Note that the first term on the right-hand side of Eq. (30) is proportional to the 2DEG density itself, not to its fluctuation. This guarantees that the Johnson-Nyquist result is valid in the equilibrium limit.

Equations (28)–(30) lead to the mean-square velocity fluctuation

$$\langle (v_x - \overline{v_x})^2 \Delta f\rangle = v_{\mathrm{th}}^2 n_s + \overline{v_x}^2 n_s^* (1 - e^{-n_s/n_s^*}). \tag{31}$$

The hot-electron temperature is[6]

$$T_e(\mathcal{E}) \equiv \frac{m^*}{k_B n_s}\langle (v_x - \overline{v_x})^2 \Delta f\rangle = T + \left(\frac{1-e^{-n_s/n_s^*}}{n_s/n_s^*}\right)\frac{m^*\mu^2}{k_B}\mathcal{E}^2. \tag{32}$$

This otherwise standard result[6] now bears the factor $\Delta n_s/n_s$ due to 2DEG degeneracy. At large n_s and/or small T, the factor produces a substantial reduction in T_e, since it is thermodynamically costly to scatter carriers out of the filled Fermi sea into the empty higher-energy states of the band. This renders the 2DEG resistant to field-induced heating. In the low-density–high-temperature limit, the degeneracy factor goes to unity and the classical result holds.

Figure 5 shows the 2DEG hot-electron temperature calculated for ambient temperature $T = 300$ K. In addition to the classical limit, we show T_e for a pseudomorphic channel at density 10^{12} cm^{-2} without the screening-induced suppression γ_s, and $\widetilde{T}_e = \gamma_s T_e$ for the same system. Degeneracy on its own reduces the value of T_e at fields above 5 kV cm^{-1}. Screening, however, produces a surprising decrease in the hot-electron temperature $\widetilde{T}_e$ at *all* values of the driving field, including equilibrium.

For a quantum-well-confined HEMT channel at room temperature, the system fluctuates as if it were an unconfined free-electron fluid cooled almost to liquid-nitrogen temperatures. This has a corresponding effect on the device noise figure as we show below.

The dynamical Boltzmann-Green function $\mathcal{R}$ is computed by defining its Laplace transform

$$\hat{\mathcal{R}}_{\sigma\sigma'}(\mathbf{k},\mathbf{k}';s) = \int_0^{\infty} dt e^{-st}\mathcal{R}_{\sigma\sigma'}(\mathbf{k},\mathbf{k}';t) \tag{33}$$

and solving the transformed Eq. (10). A set of dynamical expectation values, analogous to but more complex than the moments in Eqs. (28)–(30) follows after some algebra:[28]

$$\langle\langle \Delta \hat{f}^{(2)}(s)\rangle\rangle' = \frac{\langle \Delta f\rangle}{s}, \tag{34}$$

$$\langle\langle v_x \Delta \hat{f}^{(2)}(s)\rangle\rangle' = \langle\langle v_x' \Delta \hat{f}^{(2)}(s)\rangle\rangle' = \overline{v_x}\frac{\langle \Delta f\rangle}{s}, \tag{35}$$

$$\langle\langle v_x v_x' \Delta \hat{f}^{(2)}(s)\rangle\rangle' = \frac{\tau}{1+\tau s}\left(\langle v_x^2 \Delta f\rangle + \overline{v_x}\frac{\langle v_x \Delta f\rangle}{\tau s}\right). \tag{36}$$

These, with Eqs. (28)–(30) above, determine the diffusion constant $\hat{D}_{xx} = \tau(v_{\mathrm{th}}^2 + \mu^2\mathcal{E}^2\Delta n_s/n_s)/(1+\tau^2\omega^2)$, where the Laplace transform is continued into the frequency domain $s = -i\omega$.

Finally, the noise temperature, on substituting for $\hat{D}_{xx}$ and μ in Eq. (15) and recalling Eq. (32), is

$$T_n(\omega,\mathcal{E}) = \frac{T_e(\mathcal{E})}{1+\tau^2\omega^2}. \tag{37}$$

The noise temperature clearly carries the pronounced effects of screening and degeneracy.

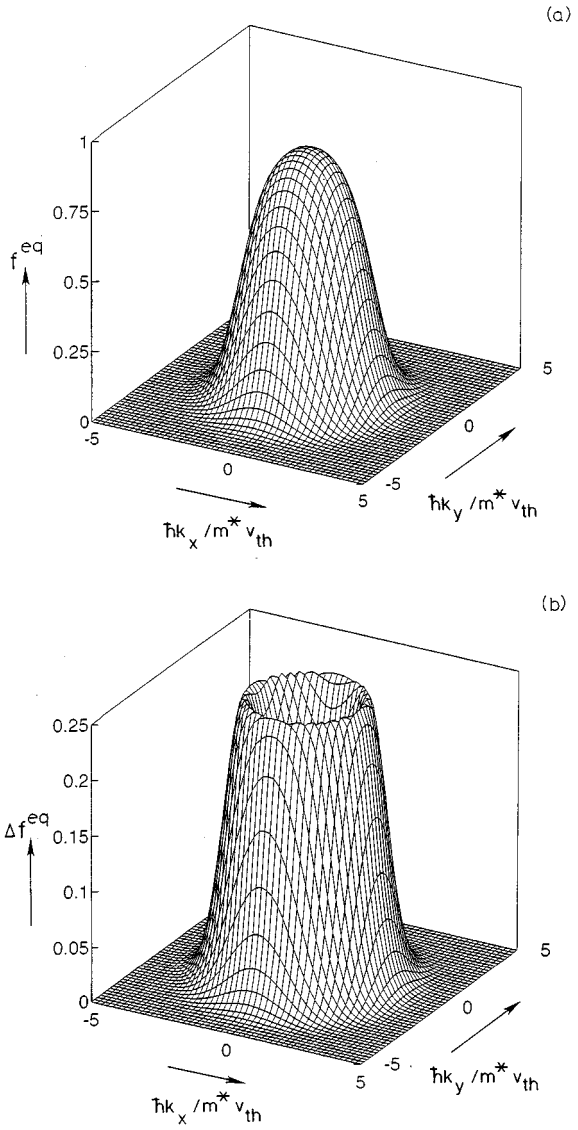

FIG. 3. (a) Fermi-Dirac distribution and (b) its fluctuation, at a density 10^{12} cm^{-2}; note the structure in Δf^{eq} around the Fermi surface. Degeneracy implies $\Delta f^{\mathrm{eq}}=f^{\mathrm{eq}}(1-f^{\mathrm{eq}})$.

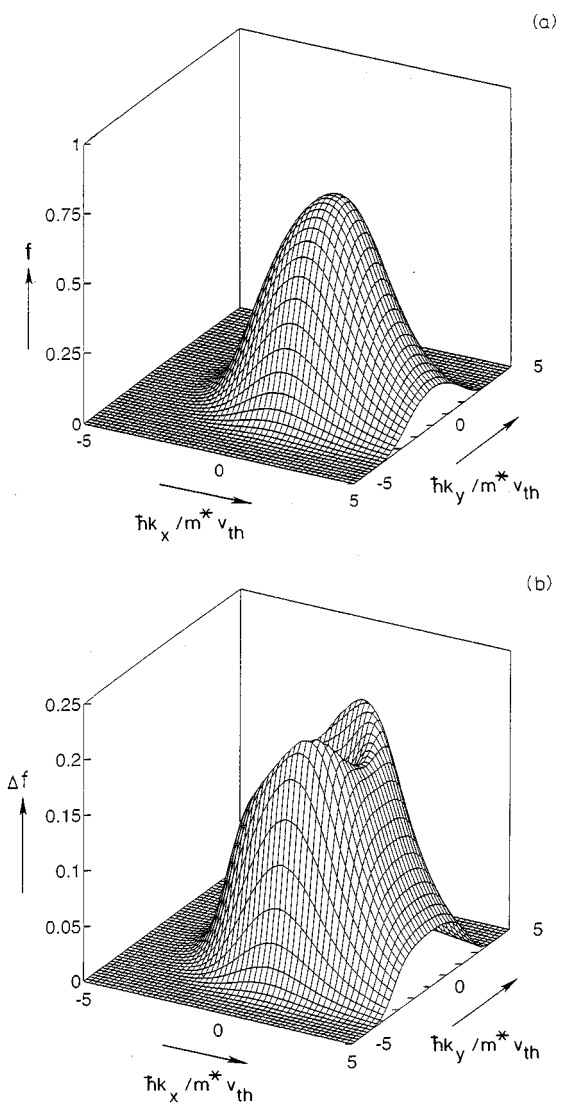

FIG. 4. (a) Degenerate nonequilibrium distribution and (b) its fluctuation, as in Fig. 3 but with a driving field of 5 kV cm^{-1} in the x direction. A strongly asymmetric remnant Fermi-surface structure is visible in Δf. The relation $\Delta f=f(1-f)$ no longer holds.

B. Microscopic structure of the device noise figure

Tke kinetic description of fluctuations in a quantum-confined 2DEG correlates strongly with measured HEMT noise, which we now examine. Our treatment here is sufficient for a preliminary, semiquantitative demonstration of core concepts. For more complete treatments of circuit-theoretical aspects, we refer to the literature.[4,16,17]

The device noise figure $F(\omega)$ is a measure of quality that reflects the incremental loss of signal purity due to the microscopic fluctuation processes in the channel.[4,16] It is defined as the quotient of the input signal-to-noise ratio and its corresponding output ratio. Since the 2DEG always adds to the amplified input noise, the noise figure always exceeds unity, but it can be minimized by tuning the external input impedance, then taking the form[28]

$$F_{\min}(\omega)=1+2\frac{\omega C_{sg}}{g_m}\sqrt{g_a(R_s+R_g+\widetilde{R}_{ch})}. \tag{38}$$

Here R_s is the nominal access resistance of the 2DEG channel on the source side, R_g is the resistance of the gate metal, and $g_a=1/(R_s+R_d)$ is the net nominal access conductance (R_d is the access resistance on the drain side of the channel). Most significantly, the minimum noise figure contains $\widetilde{R}_{ch}$, which is the apparent Nyquist-noise resistance of the active 2DEG under the gate, defined in terms of Eqs. (22) and (37):

$$\widetilde{R}_{ch}\equiv\frac{\widetilde{T}_n}{T}R_{ch}, \tag{39}$$

where R_{ch} is the conventional resistance of the active region. $\widetilde{R}_{ch}$ bears the explicit signature not only of the dynamic high-field current fluctuations in the active region but also of quantum-confined suppression. It is the nexus between our formalism and observable noise behavior.

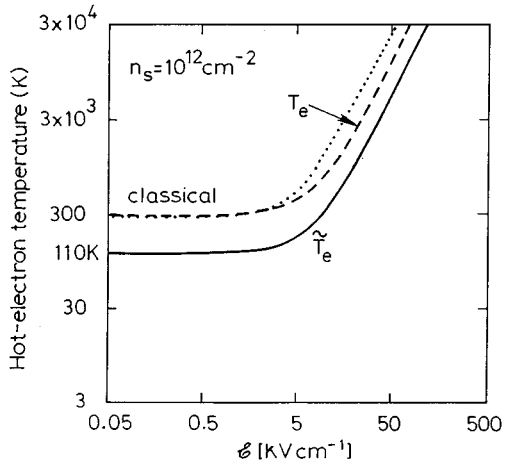

FIG. 5. Hot-electron temperature T_e for 2DEG in $In_{0.15}Ga_{0.85}$ quantum well, for ambient temperature 300 K and mobility 8000 $cm^2\ V^{-1}\ s^{-1}$. The energy gain from the electric field dominates beyond 5 kV cm^{-2}. Dots, low-density classical result; dashes, T_e at density 10^{12} cm^{-2}, without screening suppression (at high driving fields, degeneracy reduces heating rate below classical); full line, $\tilde{T}_e = \gamma_s T_e$ including screening suppression. Equilibrium fluctuations are at 110 K, not 300 K. Thus quantum confinement at room temperature reduces noise as effectively as cryogenic cooling.

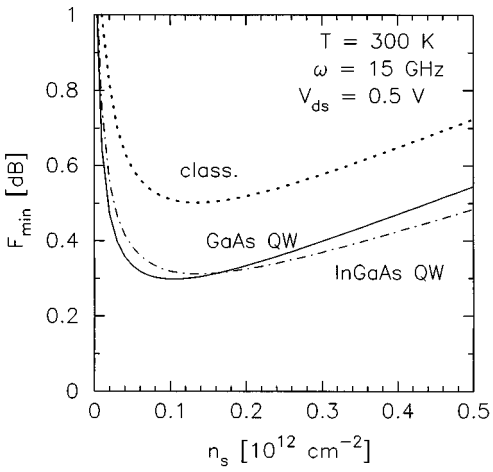

FIG. 6. Effect of microstructure on HEMT noise performance: minimum noise figure as a function of gate-modulated channel density. See the text for device specifications. Dots, classical 2DEG, equivalent to a bulk FET with the same doping-thickness product; full line, GaAs quantum-well HEMT; dot-dashed line, $In_xGa_{1-x}As$ quantum-well HEMT. The marked lowering of the noise figure for heterostructures is caused by screening-induced suppression of fluctuations in the channels' source and drain regions.

The expression for $F_{\min}$ can be brought into conventional form by rewriting it as

$$F_{\min}(\omega) = 1 + K\frac{\omega C_{sg}}{g_m}\sqrt{g_m(R_s+R_g+R_{ch})}, \qquad (40)$$

where K is given by

$$K = 2\sqrt{\frac{g_a}{g_m}\left[1+\frac{R_{ch}}{R_s+R_g+R_{ch}}\left(\frac{\tilde{T}_n}{T}-1\right)\right]}. \qquad (41)$$

The structures of Eqs. (40) and (41) lead to two fundamental points.

The first point is that K^2 is essentially the noise parameter P met in standard field-effect transistor (FET) modeling.[16,17] The presence of $\tilde{T}_n$ gives P its microscopic definition, in accord with the original FET analysis of Pucel *et al.*,[16] except that, in our model, transport and fluctuations are closely coupled by kinetic theory.

Equation (41) fixes the microscopic form of the empirical Fukui noise coefficient.[17] Its detailed numerical behavior depends (a) on how scattering is represented and (b) on how the channel's local density profile is modeled. Within the constant-mobility approximation, it is not surprising that K as a function of current does not follow Fukui's empirical law; this should emerge from a fuller description of the collision processes. However, the structure of Eq. (41) already demonstrates that hot-electron dynamics and confinement must both appear in a unified, microscopic way.

The second point is that the low-field access regions, which, in a FET, are sources of Nyquist noise, behave very differently in a HEMT. We have established that the fluctuations are strongly suppressed even at equilibrium; a more detailed analysis of Eq. (38) (Ref. 28) shows that suppression markedly decreases the noise resistance in the access regions, much as R_{ch} is changed in the active region [see Eq. (39)]. Writing $\tilde{T}_n = \gamma_s^{(0)} T$, where $\gamma_s^{(0)}$ is evaluated for the 2DEG in the access areas, the apparent Nyquist resistances become $\tilde{R}_{s,d} = \gamma_s^{(0)} R_{s,d}$. Correspondingly, the net noise conductance becomes $\tilde{g}_a = \gamma_s^{(0)} g_a$. These quantities replace R_s and g_a in Eq. (38). In fact, suppression of the access noise, an inherently quantum phenomenon, is numerically dominant in $F_{\min}$ for some ranges of the HEMT operating point, as we now show.

IV. RESULTS

In this section we analyze the microscopic effect on the HEMT noise figure, of adopting different epitaxial structures.[28] To bring the model of Sec. III closer to real devices, we add external terms to R_s and R_d in Eq. (38). This changes both the steady-state current response and the access-region noise. For example, an extrinsic resistance $R_{\rm ex}$ in series with the access region changes its electrical conductance to $g_a = 1/(R_s+R_d+R_{\rm ex})$, while its noise conductance becomes $\tilde{g}_a = [\gamma_s^{(0)}(R_s+R_d)+R_{\rm ex}]/(R_s+R_d+R_{\rm ex})^2$. In a quantum-well-confined HEMT channel, $\tilde{g}_a$ is always smaller than its FET analog, since $\gamma_s^{(0)} \sim 0.3$ (see Fig. 1).

We have calculated $F_{\min}$ as a function of active-channel density n_s, for fixed drain-to-source voltage $V_{ds} = 0.5$ V, for the following structures: (a) a classical 2DEG (in essence a FET), (b) an $Al_{0.23}Ga_{0.77}As/GaAs$ heterostructure, and (c) an $Al_{0.23}Ga_{0.77}As/In_{0.15}Ga_{0.85}As/GaAs$ pseudomorphic heterostructure.

Figure 6 shows $F_{\min}$ plotted in decibels for each device. The donor depletion and heterojunction properties are those of a triangular quantum well.[5] For the pseudomorphic example, the well is piecewise triangular with strain and

effective-mass corrections. In every case the device parameters and electrical values are the same and typical of production devices at room temperature: $\mu = 3500$ cm^2 V^{-1} s^{-1}, $R_{ex} = 20\ \Omega$ and $R_g = 5\ \Omega$, source and drain channel lengths each 1 μm, gate length 0.5 μm, and channel width 125 μm. The frequency is 15 GHz. The gate-region density n_s is bounded above by the access-region density, which is close to the maximum attainable in each quantum-well structure.

There is a pronounced density dependence in $F_{\min}$. The most striking feature is the lowering of the optimal $F_{\min}$ by 40% — from 0.50 dB to 0.30 dB — in going from the classical FET-like structure with no quantization to the full HEMT structures. Our estimate of 40% is in remarkably good agreement with the ratio of actual noise figures measured for comparable HEMTs and GaAs FETs, at frequencies ~ 15 GHz.[1]

The comparison between standard and pseudomporphic structures in Fig. 6 does not show a significant difference in optimal $F_{\min}$, but the wider valley and the minimum at $n_s = 0.14 \times 10^{12}$ cm^{-2} (rather than at $n_s = 0.10 \times 10^{12}$ cm^{-2} for GaAs) manifest the higher current-carrying capacity of the $In_xGa_{1-x}As$ well.

Our results for fluctuations in quantum-confined 2DEG's challenge the conventional view that low-noise figures in HEMT's are due to enhanced 2DEG mobility in the access regions. High mobility is indeed dominant at cryogenic temperatures, where the phonons are frozen out and the $Al_xGa_{1-x}As$ spacer layer reduces impurity scattering greatly. But the dramatic drop in the noise figure, in moving from FET to HEMTs in Fig. 6, is primary evidence that enhanced mobility cannot account for low HEMT noise, certainly not at room temperature where phonon scattering limits μ to about 8000 cm^2 V^{-1} s^{-1} in even the purest samples.

The key to HEMT noise performance must lie within the microstructure, namely, quantum confinement and the attendant suppression of current fluctuations. Figure 7 provides a specific demonstration of this. We show the GaAs-well HEMT model of Fig. 6 with the suppression factor $\gamma_s^{(0)}$ in the access regions set artificially to unity; the optimum $F_{\min}$ rises from 0.30 dB to 0.43 dB. This is compared with the classical FET of Fig. 6, whose mobility is now set to the unrealistically high room-temperature value of 8000 cm^2 V^{-1} s^{-1}; its optimum $F_{\min}$ goes down from 0.50 dB to 0.30 dB.

In other words, at room temperature a very ordinary GaAs HEMT is as good as an extraordinary (and unmanufacturable) metal-semiconductor FET. The clear reason for this is quantum-well confinement. This has strong implications for low-noise device engineering, suggesting that design emphasis should be at least as much on enhancing confinement, as on enhancing mobility.

We have also checked the effect of turning off suppression in the active region only; $F_{\min}$ rises by just 0.05 dB, rather than by 0.13 dB as for the GaAs HEMT in Fig. 7. The marked sensitivity of the noise figure to fluctuations in the access regions, compared with the influence of the high-field region, fits the observation that HEMT noise is relatively less governed by high-field effects than is the case for a FET.[29] This reflects the low density of hot electrons in relation to the carrier-rich, strongly screened, access regions.

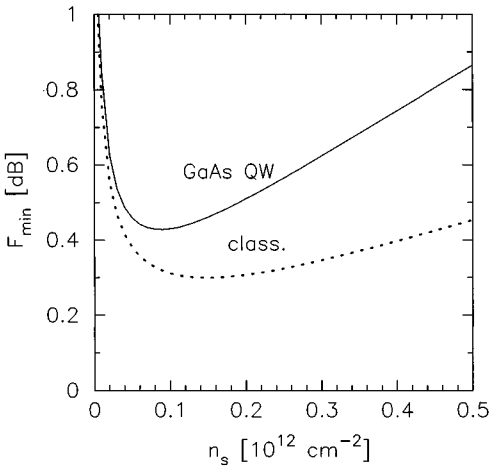

FIG. 7. Direct numerical evidence that screening suppression, not high mobility, determines low HEMT noise. Full line, GaAs heterostructure of Fig. 6 with the screening in the access regions artificially removed (the optimal $F_{\min}$ rises from 0.30 dB to 0.43 dB). Dots, classical 2DEG of Fig. 6 with mobility artificially exaggerated (the optimal $F_{\min}$ drops from 0.50 dB to 0.30 dB).

In connection with the evidence of Figs. 6 and 7, it is interesting to consider the recent paper of Feng *et al.*,[30] indicating that specially designed ion-implanted FETs can reach noise levels as low as in a pseudomorphic HEMT. We suggest that their results are not inconsistent with our own HEMT noise theory and that their low-noise figures may be explained by boundary-scattering-dominated behavior in the ultrathin FET channel, as in the theory of Bulashenko and Kochelap[31] for Nyquist noise in a constricted 2DEG.

V. CONCLUSION

We have constructed a unified and calculable microscopic theory of nonequilibrium transport and current noise in two-dimensional metallic conduction bands. Using a basic form of this theory we have detailed the microscopics of the HEMT noise figure. Quantization, not high mobility, is the inhibitor of fluctuations and the main reason for low noise. This interpretation of HEMT behavior presents a quite different perspective on low-noise design, stressing the dominance of quantum-well confinement.

Unlike the quasiempirical device models, our theory relies on microphysical parameters rather than on circuit-based parameters, which change from case to case. Our approach has predictive potential and is able to assess a wide range of heterostructures for their impact on noise. The derivation of dynamical noise properties and transport coefficients from a single, microscopically conserving formalism is also a conceptual advantage.

Our Boltzmann-Green-function method for metallic electrons, developed in analogy with the classical theory of Stanton and Wilkins, shares with that model the capacity to describe intervalley and real-space-transfer phenomena.[7,8] In future work, we plan to extend the present theory to nonuniform-channel calculations for realistic structures. To complete our program we must describe and evaluate intervalley carrier scattering, a dominant influence on high-field

transport and fluctuations.[7] Strongly inhomogeneous metallic channels are another topic for further investigation,[18] while the interaction between high electric and magnetic fields in the 2DEG, and the effect on semiclassical noise, is now being explored.

Stanton and Wilkins's work[7] suggests that device-noise data could be a sensitive diagnostic tool for nonequilibrium 2DEG dynamics. This reinforces our opinion that the Boltzmann-Green-function approach provides a deeper, yet practical, strategy for device physics. In addition, the theory of SW exhibits a smooth crossover from diffusion-dominated transport and noise at long length scales, to ballistic, shot-noise behavior at short scales.[8] This property is relevant to the trend towards nanometer-scale gate lithography.

We end with a glance at the status of our model within quantum-kinetic theory. The Boltzmann equation has been analyzed many times[10,19,32] as the classical limit of the equation of motion for the one-electron density matrix, which is nonlocal at short scales. Our picture of the nonequilibrium electron gas takes full account of degeneracy while continuing to view the *individual* carriers as free classical electrons, omitting quantum effects that do not affect the physics at scales longer than the Fermi wavelength.[32]

The recent papers of Špička and Lipavský[33] show how the Boltzmann equation can be reformulated to retain more quantum-dynamical detail. Since at cryogenic temperatures other collective quantum properties, besides degeneracy, can manifest themselves,[34] they should be assessed at nanometer scales.

ACKNOWLEDGMENTS

M.J.C. acknowledges key financial support from the Australian Postgraduate Research Award Scheme, the Australian Telecommunications and Electronics Research Board, and the Commonwealth Scientific and Industrial Research Organisation. F.G. is grateful to C. J. Stanton for first bringing the Stanton-Wilkins theory to his attention. We thank H.U. Baranger for detailed information on inhomogeneous Boltzmann transport and J. Szymański for data on the 2DEG local field correction. We acknowledge useful exchanges with S. Giugni, G. J. Griffiths, W. D. King, P. H. Ladbrooke, J. J. Lowke, R. Morrow, D. Neilson, and J. Thakur.

[1] K. H. G. Duh, M. W. Pospieszalski, W. F. Kopp, P. Ho, A. A. Jabra, P-C. Chao, P. M. Smith, L. F. Lester, J. M. Ballingall, and S. Weinreb, IEEE Trans. Electron Devices **ED-35**, 249 (1988).

[2] A collection of papers on HEMT modeling for circuit design is found in *Modulation-Doped Field-Effect Transistors: Principles, Design, and Technology*, edited by H. Daembkes (IEEE, New York, 1991). For more physics-oriented viewpoints, see *Compound Semiconductor Device Modelling*, edited by C. M. Snowden and R. E. Miles (Springer, London, 1993).

[3] Some fundamental FET-noise papers are collected within *Low-Noise Microwave Transistors & Amplifiers*, edited by H. Fukui (IEEE, New York, 1981), pp. 128–250.

[4] A. Cappy, in *Compound Semiconductor Device Modelling* (Ref. 2), pp. 194–209.

[5] F. Green, Aust. J. Phys. **46**, 447 (1993).

[6] C. J. Stanton and J. W. Wilkins, Phys. Rev. B **35**, 9722 (1987).

[7] C. J. Stanton and J. W. Wilkins, Phys. Rev. B **36**, 1686 (1987).

[8] C. J. Stanton, Ph.D. thesis, Cornell University, 1986 (unpublished).

[9] W. R. Frensley, Rev. Mod. Phys. **62**, 745 (1990).

[10] G. D. Mahan, Phys. Rept. **145**, 251 (1987).

[11] C. M. Van Vliet, IEEE Trans. Electron Devices **41**, 1902 (1994).

[12] L. Reggiani, in *Hot-Electron Transport in Semiconductors*, edited by L. Reggiani (Springer, Berlin, 1985), p. 7ff.

[13] C. Jacoboni and P. Lugli, *The Monte Carlo Method for Semiconductor Device Simulation* (Springer, Vienna, 1989).

[14] L. Varani, L. Reggiani, T. Kuhn, P. Houlet, J. C. Vaissière, J. P. Nougier, T. González, and D. Pardo, in *Noise in Physical Systems and 1/f Fluctuations*, edited by P. H. Handel and A. L. Chung, AIP Conf. Proc. No. 285 (AIP, New York, 1993), pp. 329–332.

[15] An application of stochastic Boltzmann-transport methods to FET response, including noise, is contained in C. Moglestue, IEEE Trans. Comput. Aided Design **CAD-5**, 326 (1986).

[16] R. A. Pucel, H. A. Haus, and H. Statz, *Advances in Electronics and Electron Physics* (Academic, New York, 1974), pp. 195–265.

[17] H. Fukui, IEEE Trans. Microwave Theory Tech. **MTT-27**, 643 (1979); IEEE Trans. Electron Devices **ED-26**, 1032 (1979).

[18] H. U. Baranger and J. W. Wilkins, Phys. Rev. B **30**, 7349 (1984); **36**, 1487 (1987).

[19] L. P. Kadanoff and G. Baym, *Quantum Statistical Mechanics* (Benjamin, Reading, MA, 1962).

[20] C. Kittel, *Elementary Statistical Mechanics* (Wiley, New York, 1958).

[21] G. Rickayzen, *Green's Functions and Condensed Matter* (Academic, London, 1980).

[22] J. P. Nougier, in *Physics of Nonlinear Transport in Semiconductors*, edited by D. K. Ferry, J. R. Barker, and C. Jacoboni (Plenum, New York, 1980), p. 415ff; see also J. P. Nougier, IEEE Trans. Electron Devices **41**, 2034 (1994).

[23] This result can also be understood from energetics. The total thermal energy of a density fluctuation is $k_B T$. This is made up of a kinetic term, say ΔU, and a potential term $(\delta E_0/\delta E_F)\Delta U$. The effective temperature simply measures the kinetic energy of the fluctuation $\widetilde{T}=\Delta U/k_B=T/(1+\delta E_0/\delta E_F)$.

[24] B. I. Bleaney and B. Bleaney, *Electricity and Magnetism* (OUP, London, 1976), pp. 688 and 689.

[25] S. Tedja, J. Van der Spiegel, and H. H. Williams, IEEE Trans. Electron Devices **41**, 2069 (1994).

[26] D. Neilson, L. Świerkowski, A. Sjölander, and J. Szymański, Phys. Rev. B **44**, 6291 (1991).

[27] Note that our definitions of C_{sg} and g_m include *only* the contributions from charging and transport within the 2DEG and not the parasitic terms from undepleted carriers in the $Al_xGa_{1-x}As$ donor layer; this is valid in the limit of low channel densities, when the donor layer is fully depleted. We will present a general discussion of parasitic effects in future work.

[28] F. Green and M. J. Chivers, CSIRO Radiophysics Report No. RPP3772, 1995 (unpublished).

[29] T. M. Brookes, IEEE Trans. Electron Devices **ED-33**, 52 (1986).

[30] M. Feng, D. Scherrer, J. Kruse, P. J. Apostolakis, and J. R. Middelton, IEEE Electron Device Lett. **16**, 139 (1995).
[31] O. M. Bulashenko and V. A. Kochelap, J. Phys. Condens. Matter **5**, L469 (1993); O. M. Bulashenko, in *Noise in Physical Systems and 1/f Fluctuations* (Ref. 14), pp. 23–26.
[32] B. Y.-K. Hu and J. W. Wilkins, Phys. Rev. B **41**, 10 706 (1990).
[33] V. Špička and P. Lipavský, Phys. Rev. Lett. **73**, 3439 (1994); Phys. Rev. B **52**, 14 615 (1995).
[34] T. Ando, A. B. Fowler, and F. Stern, Rev. Mod. Phys. **54**, 437 (1982).